Mon. Not. R. Astron. Soc. **391,** 447–456 (2008) doi:10.1111/j.1365-2966.2008.13917.x

Optical polarization study in the open cluster NGC 6250⋆

Carlos Feinstein,[1,2,3]† M. Marcela Vergne,[1,2,3] Ruben Martínez[1,3] and Ana María Orsatti[1,2,3]

[1]*Facultad de Ciencias Astronómicas y Geofísicas, Observatorio Astronómico, Paseo del Bosque, 1900 La Plata, Argentina*
[2]*Member of Carrera del Investigador Científico, Conicet, Argentina*
[3]*Instituto de Astrofísica de La Plata, Conicet, Argentina*

Accepted 2008 September 5. Received 2008 September 4; in original form 2008 July 11

ABSTRACT

We present (*UBVRI*) multicolour linear polarimetric data for 32 of the brightest stars in the area of the open cluster NGC 6250, with the aim of studying the properties of the interstellar medium (ISM) towards the cluster. Our data yield a mean polarization $\bar{P}_V = 1.83$ per cent, close to the polarization value produced by the ISM with normal efficiency for a mean colour excess of $E_{B-V} = 0.37$. Our analysis indicates that the observed visual absorption in NGC 6250 is caused by a nearby dust layer (within 300 pc) producing a polarization with an angle close to the Galactic plane ($\theta_{\rm GP} \sim 38^\circ$). In addition, there are at least two more dust layers along the line of sight between the Sun and the cluster producing a change in the observed polarization, making our results compatible with Neckel and Klare's results. The observations show differences between the orientation of the local magnetic field of the nearby dust layer and the one that is polarizing along the way to the cluster ($\Delta\theta_v = 20^\circ$). The internal dispersion of the polarization values for the members of NGC 6250 seems to be compatible with the presence of intracluster dust. The majority of observed stars do not present evidence of intrinsic polarization in their light. In this work, we also show (as in several previous papers) how polarimetry is an excellent technique for identifying non-member stars.

Key words: dust, extinction – open clusters and associations: individual: NGC 6250.

1 INTRODUCTION

NGC 6250 ($l = 340\overset{\circ}{.}8$ and $b = -1\overset{\circ}{.}8$) is a young open cluster, lying in a heavily obscured region within the boundaries of the next inner (Sag-Car) spiral feature. There are several arguments which suggest that the cluster is associated with the prominent dust cloud seen to the east of it. Two cluster members illuminate a reflection nebula, and other stars on the eastern side of the cluster display a larger than average reddening, indicating their own close association with substantial amounts of dust.

Moffat & Vogt (1975) presented Johnson *UBV* measurements for some members of this cluster. The most thorough study published on NGC 6250 is from Herbst (1977, hereafter HW). His observational program was undertaken for determining the extinction law in a dense dust cloud, NGC 6250 being a good candidate. The cluster was found to be affected by differential reddening with a mean extinction of $E_{B-V} = 0.37$ mag. Its age may be estimated as 1.4×10^7 yr and it is at a distance of about 1025 pc. Bayer et al. (2000) also studied this object, but their purpose was to search for chemically peculiar stars in open clusters using CCD photometry. In NGC 6250, they found two peculiar type 2 stars (according to the definition by Preston 1974) and two λ Bootis candidates. In addition, they state that effects of differential extinction are not negligible in NGC 6250.

Due to the fact that NGC 6250 is located in a dust-rich region, it is an appropriate object on which to carry out studies on interstellar polarization. This kind of research is important for three reasons: it provides information on the dust itself, it is a means to trace the Galactic magnetic field, and it is also useful in establishing membership. A comparison between polarization and extinction data in the same lines of sight provides tests for models of extinction and alignment of the grains. As they are thought to align so that their longest axes tend to become orthogonal to the direction of the local magnetic field, the observed polarization vectors map the mean field direction projected on the plane of the sky. This allows us to investigate the structure of both the macroscopic field in our Galaxy (Mathewson & Ford 1970; Axon & Ellis 1976) and the local field associated with the individual clouds (Goodman et al. 1990).

The polarimetric technique is a very useful tool for obtaining significant information (magnetic field direction, $\lambda_{\rm max}$, $P_{\rm max}$, etc.) about

⋆Based on observations obtained at Complejo Astronómico El Leoncito (CASLEO), operated under agreement between the Conicet and the National Universities of La Plata, Córdoba, and San Juan, Argentina.
†E-mail: cfeinstein@fcaglp.unlp.edu.ar

dust located in front of a luminous object. In particular, young open clusters are very good candidates to carry out polarimetric observations because previous photometric and spectroscopic studies of these clusters have provided detailed information on the colour and luminosity of the main-sequence stars of the cluster. Thus, we can compute the physical parameters of the clusters (age, distance, extinction, membership, etc.) and then, with the polarimetric data, we can study the location, size and efficiency of the dust grains to polarize the starlight and the different directions of the galactic magnetic field along the line of sight to the cluster. As the open clusters spread over some area, the evolution of the physical parameters of the dust at many location over the region can be analysed. Additionally, the polarimetric data can be used as a powerful criterion for determining the membership in a galactic cluster (e.g. Feinstein et al. 2003a) and for detecting the location of any energetic phenomenon that may have occurred in the history of a cluster (Feinstein et al. 2003b).

In this paper, we report the multicolour (*UBVRI*) measurements of linear polarization vectors for stars observed in the direction of NGC 6250. We have studied the characteristics ($P_{\max}, \lambda_{\max}$, polarization efficiency, etc.) of the dust located along the line of sight to the region where the cluster is situated. In the next sections, we will discuss the observations, the data calibrations and the results of both the individual stars and cluster as a whole.

2 OBSERVATIONS AND DATA REDUCTION

Data on linear optical polarimetry were obtained during four observing runs at the Complejo Astronómico El Leoncito (CASLEO) in San Juan, Argentina, in 2004 and 2005. We observed a sample of 32 stars and the observations were carried out using the Torino five-channel photopolarimeter (Scaltriti 1994) attached to the 2.15-m telescope. Each star was observed simultaneously through the Johnson-Cousins broad-band *UBVRI* filters ($\lambda_{U_{\rm eff}} = 0.360\,\mu$m, $\lambda_{B_{\rm eff}} = 0.440\,\mu$m, $\lambda_{V_{\rm eff}} = 0.530\,\mu$m, $\lambda_{R_{\rm eff}} = 0.690\,\mu$m and $\lambda_{I_{\rm eff}} = 0.830\,\mu$m). Standard stars for null polarization and for the zero point of the polarization position angle were observed several times each night for calibration purposes.

The polarimetric observations are listed in Table 1 which give the stellar identification from HW, the polarization percentage average (P_λ) and the position angle of the electric vector (θ_λ) through each filter, along with their respective mean errors computed as described by Maronna, Feinstein & Clocchiatti (1992).

Following HW, we have observed 18 members (#1, 2, 3, 5, 6, 8, 10, 12, 13, 17, 21, 23, 25, 26, 28, 30, 34 and 35), five probable members (#7, 9, 15, 18 and 20) and nine foreground stars (#11, 16, 19, 24, 27, 29, 32, 33 and 37).

3 RESULTS

The sky projection of the *V*-band polarization vectors for the observed stars in NGC 6250 is shown in Fig. 1. In general, an inhomogeneous distribution of the dust is observed in the region, with a dark cloud over the east and south-east sides and a more transparent region to the south-west side. The dotted line superimposed on the figure is the galactic parallel, $b = -2.^\circ0$. In this plot, we observe three polarimetric stellar groups characterized by different alignments of the polarization vectors in relation to the Galactic plane (GP). There is a group composed of nearby non-member stars (#11, 16, 19, 23, 24, 27 and 29), which has polarization vectors orientated in the direction of the Galactic disc ($\sim 38.^\circ0$), and its stars are randomly distributed on the sky plane; and a second group composed of members and probable members with a mean polarization angle $\bar{\theta}_V = 19.^\circ7$, the majority of them lying in the central region of the cluster. Finally, there is a third group (#2, 20, 25, 26, 28 and 33) with $\bar{\theta}_V = 8.^\circ6$, located on the south-west part of the image.

Fig. 2 displays the relation that exists between P_V and θ_V, representing with different symbols member, probable member and non-member stars according to HW. This figure shows a large dispersion in polarization angles but not the segregation into different stellar groups as was observed in other stellar clusters studied (Martínez, Vergne & Feinstein 2004; Vergne, Feinstein & Martínez 2007). No clear dependence with the polarization angle is observed in this figure; the majority of the member stars have their polarimetric orientations in the range 4°–25°, while the polarization values are between 1.5 and 2.2 per cent.

4 ANALYSIS AND DISCUSSION

4.1 Intrinsic polarization

Assuming that the polarization is of interstellar origin, the wavelength at which the maximum polarization $P_{\max}$ occurs can be computed by observing in the five photometric bandpasses mentioned (*UBVRI*). This wavelength $\lambda_{\max}$ depends on the optical properties and the distribution of the aligned grains (McMillan 1978; Wilking et al. 1980). The $P_{\max}$ and $\lambda_{\max}$, listed in Table 2, were obtained using a weighted least-squares fit of the observed interstellar polarization in the *UBVRI* bandpasses to the standard Serkowski's polarization law (Serkowski 1973):

$$P_\lambda / P_{\max} = {\rm e}^{-K \ln^2(\lambda_{\max}/\lambda).} \quad (1)$$

To perform the fitting, we adopted $K = 1.66\,\lambda_{\max} + 0.01$ (Whittet et al. 1992). These values were calculated for 29 out of the 32 stars in our sample, due to the fact that three of them (#24, 27, 30) have only data in the *V* filter. If the polarization is well represented by (equation 1) relation, σ_1 (the unit weight error of the fit, column 3 in this table) should not be higher than 1.5 because of the weighting scheme; a much higher value could indicate the presence of intrinsic polarization (see the mathematical expression in Table 2 as a footnote). Other criteria to detect intrinsic stellar polarization come from computing the $\lambda_{\max}$ value and analysing the dispersion of the position angle for each star normalized by the average of the position angle errors ($\bar{\epsilon}$). In the first case, only stars with a $\lambda_{\max}$ much lower than the average value of the interstellar medium (ISM) (0.545 μm; Serkowski, Mathewson & Ford 1975) are candidates to have an intrinsic component of polarization.

Applying the criteria mentioned before, we find that the majority of the observed stars in the region of NGC 6250 do not present indications of intrinsic polarization. Only six stars (#11, 13, 18, 19, 35 and 37) show some evidence to be considered as a probable candidate to have an intrinsic component of polarization (Fig. 3). All of them have a significant rotation in the polarization position angle, but only three stars are mentioned in the literature for having some peculiar characteristic. Star #35 is illuminating a nearby reflection nebula, and it exhibits a B_e phenomenon (B2IV$_e$, Levenhagen & Leister 2006). Star #11, according to photometric data, has a spectral type of approximately F8V and a calculated E_{B-V} value of 0.08 mag, but according to Bayer et al. (2000) it may be a spectroscopic binary. Finally, Star #37, a non-member star, is considerably distant from the cluster (~30 arcmin to the east of the cluster) and it was observed only because it illuminates a reflection nebula which seems to be associated with the same dust cloud as NGC 6250 (HW).

Table 1. Polarimetric observations of stars in NGC 6250.

Star identification	U P_U(per cent) $\pm \epsilon_{P_U}$ $\theta_U(^\circ) \pm \epsilon_{\theta_U}$	B P_B(per cent) $\pm \epsilon_{P_B}$ $\theta_B(^\circ) \pm \epsilon_{\theta_B}$	V P_V(per cent) $\pm \epsilon_{P_V}$ $\theta_V(^\circ) \pm \epsilon_{\theta_V}$	R P_R(per cent) $\pm \epsilon_{P_R}$ $\theta_R(^\circ) \pm \epsilon_{\theta_R}$	I P_I(per cent $\pm \epsilon_{P_I}$ $\theta_I(^\circ) \pm \epsilon_{\theta_I}$
1	1.37 ± 0.16 18.8 ± 3.4	1.56 ± 0.14 18.7 ± 2.6	1.66 ± 0.19 20.9 ± 3.3	1.67 ± 0.14 18.5 ± 2.4	1.43 ± 0.16 19.6 ± 3.2
2	1.70 ± 0.15 10.1 ± 2.4	1.86 ± 0.12 6.6 ± 1.8	2.08 ± 0.09 9.0 ± 1.2	2.07 ± 0.08 7.0 ± 1.1	2.00 ± 0.14 6.3 ± 2.1
3	1.45 ± 0.16 14.9 ± 3.1	1.64 ± 0.19 14.3 ± 3.3	1.85 ± 0.24 17.3 ± 3.7	1.78 ± 0.17 15.0 ± 2.7	1.65 ± 0.25 14.7 ± 4.2
5		2.29 ± 0.39 22.8 ± 4.8	2.12 ± 0.37 24.5 ± 4.9	2.45 ± 0.48 24.5 ± 5.6	2.50 ± 0.67 27.4 ± 7.5
6		1.60 ± 0.41 19.9 ± 7.2	2.01 ± 0.34 24.1 ± 4.8	1.74 ± 0.31 22.4 ± 5.0	1.95 ± 0.34 23.4 ± 4.9
7	1.31 ± 0.26 13.3 ± 5.6	1.68 ± 0.22 22.0 ± 3.8	1.13 ± 0.22 18.4 ± 5.4	1.46 ± 0.25 18.0 ± 4.8	1.23 ± 0.33 4.9 ± 7.5
8		1.82 ± 0.16 17.3 ± 2.6	1.87 ± 0.09 14.6 ± 1.3	1.62 ± 0.11 18.9 ± 1.9	1.35 ± 0.13 10.9 ± 2.8
9	1.22 ± 0.33 15.3 ± 7.6	1.46 ± 0.20 15.0 ± 3.9	1.44 ± 0.26 19.7 ± 5.2	1.53 ± 0.16 19.3 ± 3.0	1.27 ± 0.32 12.5 ± 7.1
10		1.41 ± 0.09 15.5 ± 1.9	1.52 ± 0.05 17.3 ± 1.0	1.44 ± 0.06 19.0 ± 1.2	1.55 ± 0.09 18.6 ± 1.6
11		1.00 ± 0.13 36.1 ± 3.6	0.85 ± 0.09 49.7 ± 3.1	0.71 ± 0.09 38.8 ± 3.7	0.48 ± 0.11 24.9 ± 6.5
12		1.00 ± 0.17 16.0 ± 4.8	1.48 ± 0.12 23.5 ± 2.3	1.37 ± 0.10 20.5 ± 2.0	1.14 ± 0.16 28.9 ± 4.1
13	1.00 ± 0.20 9.3 ± 5.8	1.72 ± 0.11 20.3 ± 1.8	1.58 ± 0.11 19.3 ± 1.9	1.52 ± 0.13 19.5 ± 2.5	1.32 ± 0.37 31.8 ± 7.8
15	0.94 ± 0.22 21.7 ± 6.5	1.11 ± 0.28 27.0 ± 7.0	1.21 ± 0.22 25.1 ± 5.1	1.03 ± 0.25 25.8 ± 6.8	0.94 ± 0.38 20.9 ± 11.1
16		0.75 ± 0.13 44.0 ± 4.9	0.60 ± 0.11 40.1 ± 5.0	0.64 ± 0.09 44.3 ± 4.0	0.50 ± 0.07 42.4 ± 4.1
17	1.37 ± 0.14 12.8 ± 2.9	2.09 ± 0.16 14.4 ± 2.2	2.06 ± 0.18 16.4 ± 2.5	2.23 ± 0.17 12.5 ± 2.1	1.61 ± 0.21 17.7 ± 3.7
18	1.43 ± 0.25 7.2 ± 4.9	2.00 ± 0.22 13.7 ± 3.2	1.70 ± 0.20 14.8 ± 3.4	2.31 ± 0.14 14.7 ± 1.7	1.67 ± 0.21 20.3 ± 3.6
19	1.04 ± 0.28 25.1 ± 7.4	1.02 ± 0.21 27.3 ± 5.9	1.35 ± 0.14 41.9 ± 2.9	1.03 ± 0.14 7.4 ± 3.9	0.70 ± 0.17 13.5 ± 6.6
20	1.88 ± 0.25 3.8 ± 3.8	1.98 ± 0.22 4.8 ± 3.2	2.12 ± 0.23 4.0 ± 3.2	2.05 ± 0.23 4.5 ± 3.2	1.64 ± 0.26 6.0 ± 4.5
21	1.01 ± 0.19 12.2 ± 5.4	1.22 ± 0.17 4.5 ± 4.1	1.06 ± 0.36 7.3 ± 9.3	1.13 ± 0.31 12.4 ± 7.7	
23	1.17 ± 0.31 44.3 ± 6.0	0.78 ± 0.20 36.8 ± 5.7	0.79 ± 0.12 31.6 ± 3.5	0.72 ± 0.09 34.5 ± 2.8	
24			0.55 ± 0.07 43.8 ± 3.6		
25	1.71 ± 0.47 3.5 ± 7.6	1.93 ± 0.12 11.9 ± 1.7	1.96 ± 0.27 14.1 ± 4.0	1.87 ± 0.20 13.0 ± 3.1	1.64 ± 0.27 12.5 ± 4.7
26		1.63 ± 0.14 15.0 ± 2.4	1.78 ± 0.08 11.5 ± 1.2	1.88 ± 0.11 9.7 ± 1.7	1.50 ± 0.11 10.7 ± 2.1
27			0.58 ± 0.08 30.5 ± 3.9		
28	1.16 ± 0.25 7.1 ± 6.0	1.88 ± 0.20 4.9 ± 3.1	1.73 ± 0.20 4.3 ± 3.3	1.74 ± 0.12 0.8 ± 2.0	1.57 ± 0.16 3.1 ± 2.9
29		0.78 ± 0.25 35.2 ± 8.7	0.67 ± 0.24 42.5 ± 9.7	0.73 ± 0.17 46.7 ± 6.7	0.63 ± 0.21 44.3 ± 9.1

Table 1 – *continued.*

Star identification	U $P_U \pm \epsilon_{P_U}$ $\theta_U \pm \epsilon_{\theta_U}$	B $P_B \pm \epsilon_{P_B}$ $\theta_B \pm \epsilon_{\theta_B}$	V $P_V \pm \epsilon_{P_V}$ $\theta_V \pm \epsilon_{\theta_V}$	R $P_R \pm \epsilon_{P_R}$ $\theta_R \pm \epsilon_{\theta_R}$	I $P_I \pm \epsilon_{P_I}$ $\theta_I \pm \epsilon_{\theta_I}$
30			1.57 ± 0.10 20.2 ± 1.8		
32	0.64 ± 0.10 31.7 ± 4.6	0.66 ± 0.11 31.8 ± 4.6	0.76 ± 0.24 28.7 ± 8.9		0.69 ± 0.24 14.9 ± 9.5
33	0.82 ± 0.16 178.3 ± 5.6	1.48 ± 0.15 175.0 ± 3.0	1.77 ± 0.35 1.2 ± 5.6	2.02 ± 0.40 4.2 ± 5.6	1.93 ± 0.52 3.2 ± 7.6
34	2.33 ± 0.20 26.6 ± 2.5	2.74 ± 0.11 29.9 ± 1.1	2.86 ± 0.12 31.7 ± 1.2	2.97 ± 0.10 30.2 ± 1.0	2.43 ± 0.14 28.4 ± 1.6
35	2.09 ± 0.42 14.4 ± 5.7	1.77 ± 0.18 27.3 ± 2.9	1.92 ± 0.19 27.8 ± 2.8	1.94 ± 0.18 30.8 ± 2.7	1.68 ± 0.23 33.6 ± 3.8
37		1.62 ± 0.09 20.2 ± 1.6	1.94 ± 0.04 23.0 ± 0.6	1.84 ± 0.03 21.0 ± 0.4	1.70 ± 0.03 17.7 ± 0.5

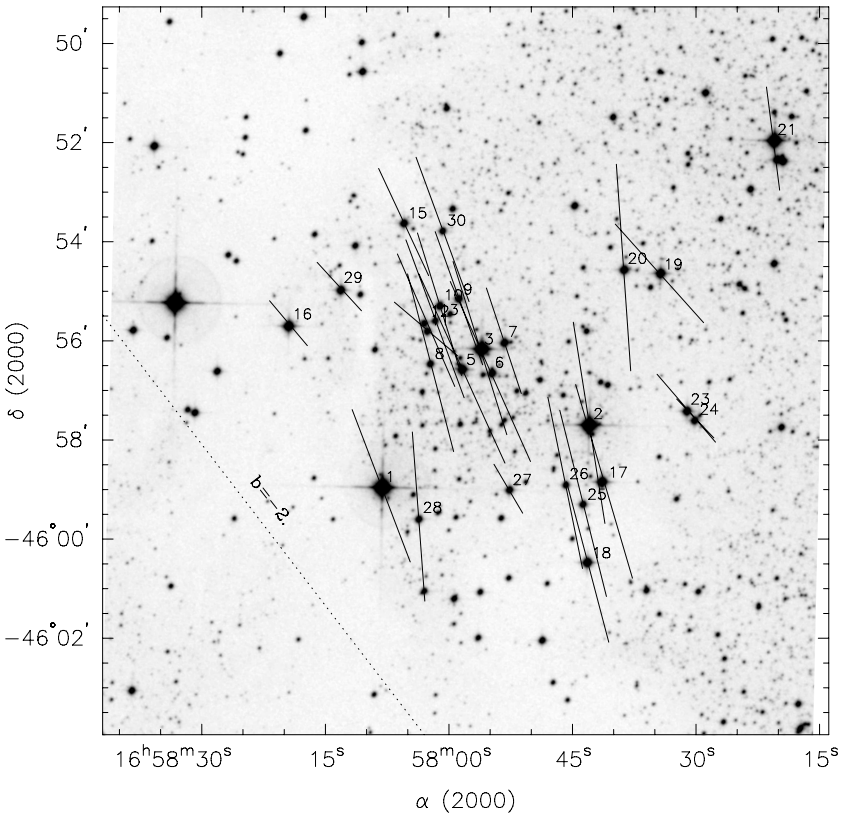

Figure 1. Projection on the sky of the polarization vectors (Johnson V filter) of the stars observed in the region of NGC 6250. The dot-dashed line is the galactic parallel, $b = -2^\circ$. This plot shows only the observed stars close to the central core.

4.2 Stokes plane

To confirm the results mentioned in Section 3, we have plotted the individual Stokes parameters of the polarization vector of the V filter $\boldsymbol{P}_V$, given by $Q_V = P_V \cos(2\theta_V)$ and $U_V = P_V \sin(2\theta_V)$ (the equatorial components of $\boldsymbol{P}_V$), for each of the observed stars (Fig. 4). This plot provides useful information on the evolution of the interstellar environments from the Sun to the cluster. In the figure, the point of coordinates $Q_V = 0$ and $U_V = 0$ represents the dustless solar neighbourhood, and any other point would indicate the direction of the polarization vector as seen from the Sun. Clearly, this figure shows that the observed stars over the region segregate into different polarimetric groups. The solid lines in Fig. 4 represent the changing direction of the vector $\boldsymbol{P}_V$ while connecting the mean (Q_V, U_V) values for the possible three different groups. The nearby group has six non-member stars (#11, 16, 24, 27, 29 and 32) and one member (#23), with a mean polarization value of 0.69 per cent and an orientation of ($\bar{\theta}_V = 38.^\circ1$). This group lies parallel to the GP

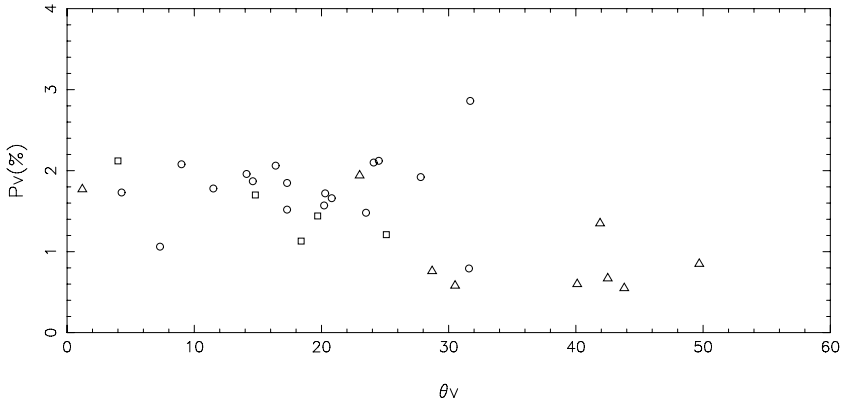

Figure 2. *V*-band polarization percentage of the stellar flux P_V (per cent) versus the polarization angle θ_V for each star. Circles indicate member stars; squares, probable members; and triangles, non-members as classified by HW.

Table 2. Parameters of the Serkowski fit to the linear polarization data for stars in NGC 6250. '?' indicates a probable member.

Stellar identification	$P_{\max} \pm \epsilon_P$ (per cent)	σ_1^c	$\lambda_{\max} \pm \epsilon_{\lambda_{\max}}$ (mμ)	$\bar{\epsilon}$	Membership	Spectral T^d
1	1.670 ± 0.022	0.295	0.573± 0.014	0.230	m	B2II-III
2	2.112 ± 0.025	0.468	0.611± 0.016	0.871	nm	B2III
3	1.821 ± 0.017	0.167	0.600± 0.009	0.270	m	B5IV
5	2.431 ± 0.169	0.568	0.650± 0.094	0.355	m	–
6	1.921 ± 0.111	0.609	0.657± 0.090	0.323	m	–
7	1.452 ± 0.132	1.116	0.504± 0.094	4.559	nm	–
8	1.889 ± 0.036	0.357	0.455± 0.014	2.771	m	–
9	1.530 ± 0.032	0.288	0.576± 0.026	1.146	nm	–
10	1.547 ± 0.044	1.212	0.623± 0.046	0.978	m	–
11	1.062 ± 0.110	0.461	0.334± 0.030	13.838	nm	–
12	1.350 ± 0.098	1.414	0.629± 0.125	3.033	nm	–
13	1.619 ± 0.147	1.811	0.692± 0.155	1.432	m	–
15	1.133 ± 0.030	0.253	0.542± 0.028	0.572	nm	–
16	0.692 ± 0.067	0.695	0.461± 0.056	0.520	nm	–
17	2.062 ± 0.177	1.623	0.645± 0.081	1.207	m	–
18	2.061 ± 0.160	1.650	0.647± 0.097	2.259	?	B8V
19	1.227 ± 0.162	1.100	0.416± 0.069	41.112	nm	A7V
20	2.097 ± 0.042	0.360	0.520± 0.020	0.119	m?	A2V
21	1.198 ± 0.063	0.396	0.535± 0.055	2.289	m?	B2V
23	0.870 ± 0.102	0.844	0.424± 0.073	1.462	nm	–
25	1.982 ± 0.006	0.067	0.528± 0.004	0.671	m	–
26	1.794 ± 0.059	1.097	0.571± 0.047	1.289	m	–
28	1.761 ± 0.081	0.925	0.603± 0.057	1.062	m	–
29	0.752 ± 0.042	0.299	0.529± 0.056	2.223	nm	–
32	0.740 ± 0.040	0.340	0.567± 0.048	3.474	nm	B9V
33	2.636 ± 0.773	1.004	1.065± 0.189	2.453	nm	B9.5V
34	2.919 ± 0.063	1.070	0.575± 0.026	1.067	nm	B2III
35[a]	1.961 ± 0.070	0.705	0.555± 0.043	5.117	m	B2IV$_e$
37[b]	1.894 ± 0.039	1.524	0.586± 0.028	5.045	nm	B1

[a]Illuminates a reflection nebula VBH 79 (Van den Bergh & Herbst 1975).
[b]Illuminates nebulosity visible on European Southern Observatory sky survey blue plate. CoD-45° 11 128.
[c] $\sigma_1{}^2 = \Sigma(r_\lambda/\epsilon_{P_\lambda})^2/(m-2)$; where m is the number of the observed filters and $r_\lambda = P_\lambda - P_{\max} \exp[-K\, ln^2(\lambda_{\max}/\lambda)]$.
[d]Spectral type from the WEBDA data base.

(dashed line). Another group consists in three probable members (#7, 9 and 15) and a member (#12) with mean polarization value of 1.32 per cent, and with a direction of $\bar{\theta}_V = 21\overset{\circ}{.}7$. But, most of the cluster stars are in other group, which has a mean polarization and orientation (considering only the members of NGC 6250: #1, 3, 5, 6, 8, 10, 13, 17, 25, 26 and 30) of 1.83 per cent and $\bar{\theta}_V = 18\overset{\circ}{.}3$, respectively. Four stars (#2, 20, 28 and 35) were excluded to calculate these mean values. Star 2 has a membership probability of 35 per cent (Baumgardt, Dettbam & Wielen 2000); therefore, it may be a non-member. Stars #20 and 28 have high errors in their angles, but their polarization values are similar to the rest of member stars. In particular, the star #20 is probably a cluster member and binary (HW), therefore it could have a non-interstellar polarization component, though our estimators of intrinsic polarization do not

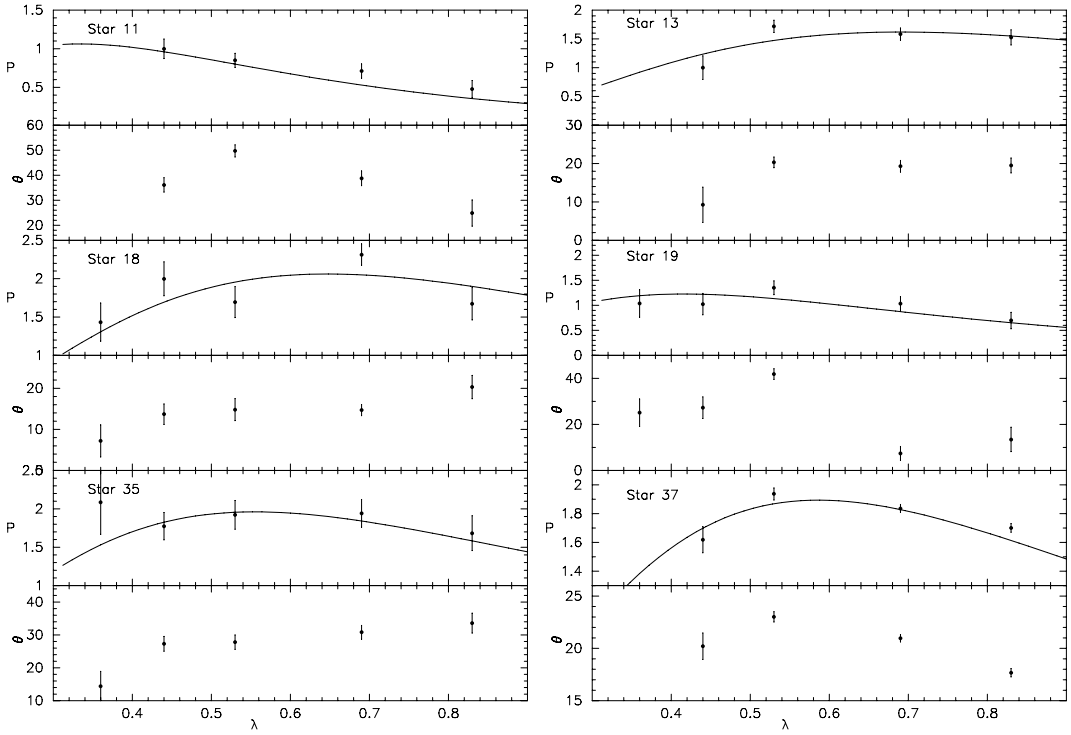

Figure 3. Polarization and position angle dependence on wavelength for probable candidates to have an intrinsic component of polarization.

show it. And the star 35, as mentioned in the preceding section, could have an intrinsic polarization component. In the upper part of the plot is situated the star #34, originally considered as member by HW, with a high polarization value (2.86 per cent), its alignment ($\theta_V = 31\overset{\circ}{.}7$) is close to the projection of the GP.

The orientation of the polarimetric vectors and their moduli show that the light from the nearby group stars to the Sun is being polarized by a close dust cloud dominated by the GP. Also, this same cloud affects the polarization of all the observed stars, including the grouping of stars #7, 9, 12 and 15, and the cluster. The difference between the mean polarization values of the four stars #7, 9, 12 and 15 and the cluster can be due to the existence of a dust cloud (or several) located between both groups. Also, there are some clues that the light from the member stars is being affected by an intracluster dust component, as was suggested by HW and Bayer et al. (2000). In our data, the evidence of the presence of intracluster dust is given by some difference in the observed polarization ($\Delta P_V = 0.6$ per cent) and in the orientation of the polarization vectors ($\Delta\theta_V = 13^\circ$).

Two stars (#19 and 21) are found out of the regions where the majority of the observed stars are located on this plane. Star 21, an original member star with spectral type B2V (Garrison, Hitner & Schild 1977), has an observed polarization of $P_V = 1.06$ per cent and an orientation of $\theta_V = 7\overset{\circ}{.}3$. Both values are lower than the mean values for the cluster, and the error in the angle ($9\overset{\circ}{.}3$) is higher than the same value. The polarimetric data of star 19 ($P_V = 1.35$ per cent and $\theta_V = 41\overset{\circ}{.}9$) confirm that it is a foreground star (HW), with polarization value similar to the group constituted by stars 7, 9, 12 and 15, but its angle is higher than for these. This star shows an important variation of its angles in function of λ (see Fig. 3). The difference between the polarization angles in the filters *V* and *R* is approximately 35°, which is quite a substantial departure from the constant angle of the polarization by the ISM (37°). The observations of the star #33 (a non-member) and the distribution of the dust on the line of sight to the cluster will be discussed in Section 4.4.

4.3 Cluster membership

The polarimetric observations are an excellent tool for determining membership in Galactic open clusters, particularly, when the field stars have colours that are similar to those of cluster members (Martínez et al. 2004; Vergne et al. 2007). This cluster can be described by the following polarimetric parameters: $P_V > 1$ per cent and $11^\circ < \theta_V < 28^\circ$. Applying these criteria, we end up with 17 stars: 13 of them were previously considered as members by HW (#1, 3, 5, 6, 8, 10, 12, 13, 17, 25, 26, 30 and 35) and four as probable members (#7, 9, 15 and 18) while the rest of the stars are non-members. Three of the probable members (#7, 9 and 15) have, according to their photometric data (HW), smaller reddenings than those of early-type cluster members (0.26, 0.29 and 0.28, respectively), but their distance moduli are comparable. HW supposed that they are probably in front of the dust cloud associated with the cluster and may or may not be the cluster members. Polarimetrically, these stars have polarization values lower than the values of the member stars, which are consistent with the lower excesses E_{B-V}, but the orientations of their polarimectric vectors are similar to those of the cluster members. So, they are probably close to the cluster along the line of sight, but are likely to be non-members. To verify this interpretation, we have plotted the colour–colour diagram (Fig. 5) using HW's data. This figure displays a sharper main sequence than the previous one from HW and shows that stars #7, 9 and 15 are probably field stars, and therefore, non-members. The three stars are seen as projected on the same region of the sky (Fig. 1). In this group of field stars are also included stars #18, 32 and 33. Star #18 is far from the main sequence, but as mentioned, it is a candidate to

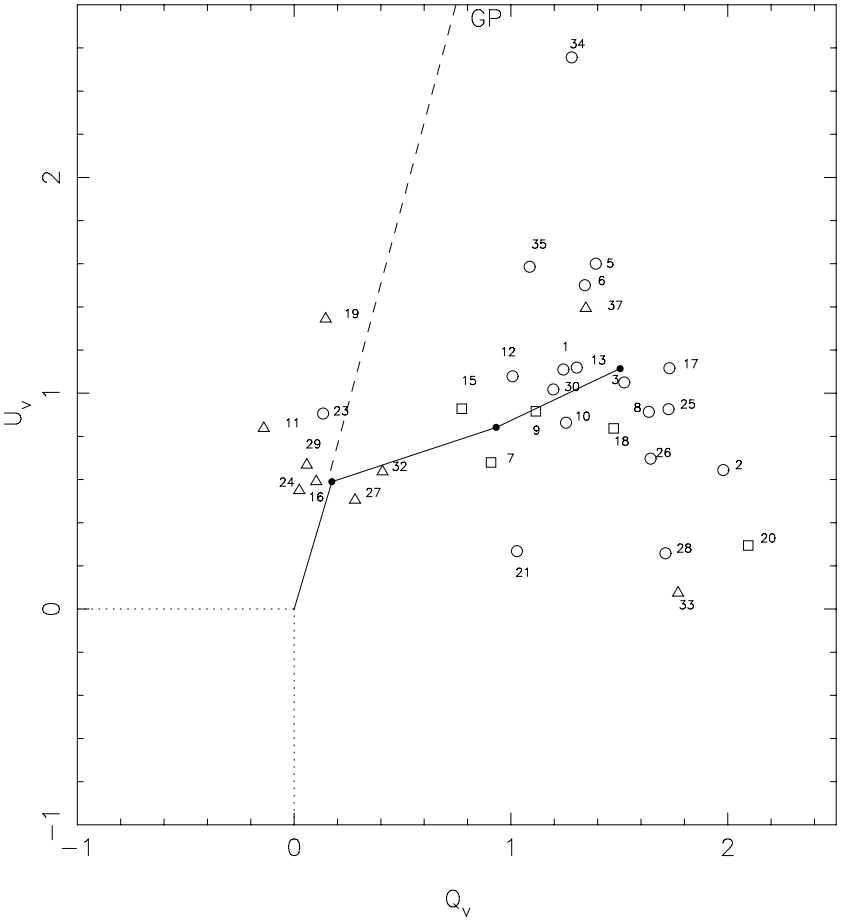

Figure 4. U_V versus Q_V plot for the stars of NGC 6520. Symbols are as indicated in Fig. 2. The dashed line is in the direction of the GP. The solid line is the interpretation of the evolution of the polarization through the dust layer between the cluster and Sun.

have an intrinsic component, therefore, in this case, we prefer not to use polarimetry as a membership criterion.

Meanwhile, star #23 has a colour excess of 0.37 mag (HW) and its colours are similar to those of cluster members. Through polarimetry, this star – a member of the near group (see Fig. 4) – shows a low polarization value of 0.79 ± 0.12, incompatible with its colour excess, and with an orientation of 31°.6. If we estimate a new colour excess value by calculating the Q parameter (Schmidt-Kaler 1982), we obtain $Q = 0.26$ mag. Therefore, star #23, according to Fig. 4, its low polarization value and colour excess, is a non-member.

Finally, star #34 (a member, according to HW) has the highest polarization value in our stellar sample. The orientation of its polarization vector is close to the projection of the GP in this region. This star is far from the main sequence and is classified as B2III (Houk, Cowley & Smith-Moore 1975). The earliest spectral class for NGC 6250 is B1, therefore, this star can be a non-member. On the sky, star #34 is located far away from the cluster on the south-east size of the nearby dust cloud. Therefore, its light is being polarized by another dust cloud, different from the one that polarizes to the cluster. According to photometric data, it is situated at about 2000 pc, with a $E_{B-V} = 0.47$ mag, while NGC 6250 is located close to 1025 pc (HW). Consequently, we are able to conclude that this star is a likely non-member. The polarimetric membership data are listed in column 7 of Table 2.

4.4 Polarization efficiency

The ratio P_V/E_{B-V} is known as the 'polarization efficiency' of the ISM, and it depends mainly on the alignment efficiency, the projection of the spatial alignment and the magnetic field strength. It also depends on the amount of depolarization due to radiation traversing more than one dust cloud with different magnetic field directions. Fig. 6 displays the relation (P_V versus E_{B-V}) that exists between the polarization and the extinction due to the dust along the line of sight to NGC 6250.

Assuming normal interstellar material characterized by $R_V = 3.2$, the empirical upper limit relation for the polarization efficiency given by $P_V = RA_V \sim 9E_{B-V}$ (Serkowski et al. 1975) is depicted by the solid line in this figure. Indeed, this line represents the empirical maximum efficiency of the polarization produced by the interstellar dust. Likewise, the dotted line $P_V = 3.5\,{E_{B-V}}^{0.8}$ represents the most recent estimate of the average efficiency made by Fosalba et al. (2002), valid for $E_{B-V} < 1.0$ mag. For comparison purposes, the dashed line $P_V = 5E_{B-V}$ was drawn as a reference for the previously accepted determination of the observed normal efficiency of the polarizing properties of dust given by Serkowski et al. (1975).

Excesses E_{B-V} were obtained from the literature or from the relation between spectral type and colour indices following Schmidt-Kaler (1982). As shown in Fig. 6, the majority of stars lie to the right of the interstellar maximum efficiency line; this indicates that

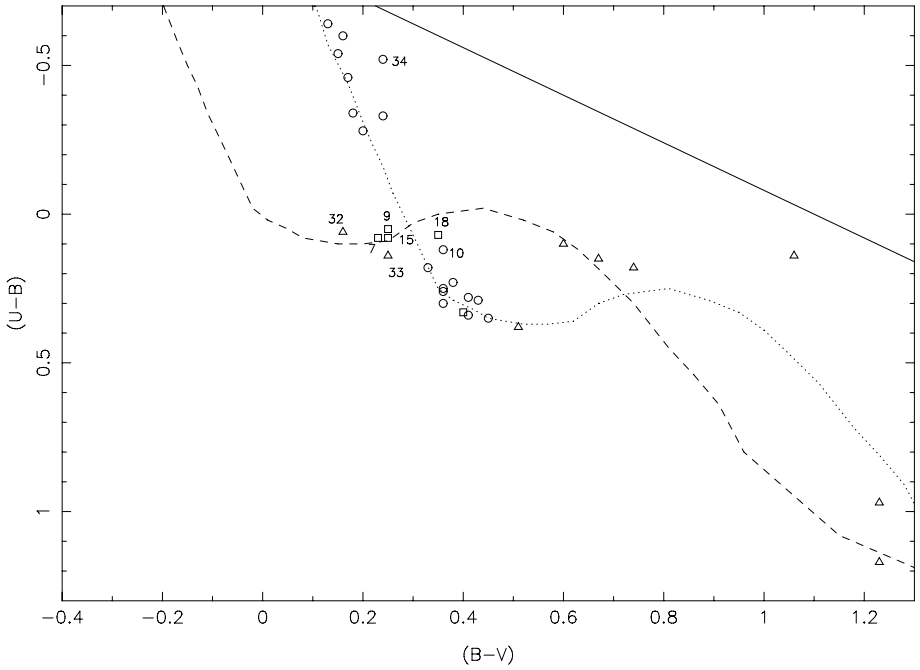

Figure 5. Remake of the colour–colour diagram for the cluster. Symbols are as indicated in Fig. 2. The dashed line is the unreddened main sequence, the dotted line is the reddened main sequence and the full line is the reddening line. Polarization criteria proved very efficient for cleaning the main sequence of field stars.

the observed polarization is mostly due to the interstellar material, except for one star (#11), which is likely intrinsically polarized (see Fig. 3).

For NGC 6250, we obtain a mean polarization efficiency of $P_V/E_{B-V} = 4.95$ (over 11 stars), appearing to be in good agreement with Serkowski's relation, but it is higher than the value predicted by Fosalba et al. (2002). The mean wavelength of the maximum linear polarization for the cluster amounts to $\bar{\lambda}_{\max} = 0.59 \pm 0.06\,\mu$m (over the same stars), close to the average value for the ISM found by Serkowski et al. (1975).

Star #29 is situated on the lower part of the plot, and it was previously identified as a non-member by HW. According to its photometric data, HW has calculated for this star an $E_{B-V} = 0.37$, but this value does not agree with its low polarization (0.75 per cent). If we estimate the colour excess from the photometry by calculating the Q parameter (Schmidt-Kaler 1982), we obtain 0.08 mag, so the star is located within 200 pc from the Sun. Therefore, this confirms that its polarization originates in the nearby dust cloud mentioned in Section 4.2, dominated by the GP, and for that reason the star would belong to the field stars. The polarimetric values for the star confirm this finding.

Star #32, together with star #29, belongs to this last group (see Fig. 4). Fig. 6 shows that this star has a normal efficiency. In the case of stars #16 and 23, HW have published excess values of 0.37 mag, not agreeing with their polarization values. When we estimate their colour excesses from the photometry data, using the Q parameter (Schmidt-Kaler 1982), we obtain 0.29 and 0.26 mag, in spite of that these values continue being high in relation to the polarization value. We think that these stars may be evolved stars or late-type stars whose excesses may be over estimated. In Fig. 6, they are marked using an arrow that points to smaller excess values.

Behind this near group of stars lies another dust cloud producing a gradual increase in polarization, and affecting the group composed of the four non-member stars (#7, 9, 12 and 15), with a normal polarization efficiency $P_V/E_{B-V} = 5.08$, similar to the observed value for the ISM. The difference in angle in comparison to the first dust component ($\Delta\theta \sim 20^\circ$) is the result of the composition with a polarization produced by dust particles oriented by a magnetic field with a different angle. These non-member stars are located, according to photometric data, within 600 pc from the Sun. In front of the cluster, behind the group of four stars (#7, 9, 12 and 15), the polarization increases gradually again due to the presence of another dust cloud, confirming the information given in Section 4.2.

In the case of the cluster NGC 6250, it is interesting to observe in the figure the presence of scattering in E_{B-V} and P_λ. One possible explanation for this scatter could be the existence of a dust component located inside the cluster, as suggested in Fig. 4. Neckel & Klare (1980) have computed the growth of A_V with increasing distance in the area of NGC 6250. Their figure (fig. 6j-209) displays that the absorption increases gradually from the Sun at a maximum distance of 300 pc, with an increase in extinction up to $A_V \sim 0.5$. This is in very good agreement with the mean $\bar{E}_{B-V}$ calculated for the first non-member star group, and with a range in distance for the first dust cloud within 300 pc. Further away, the absorption remains constant between 300 and 700 pc, where stars #7, 9, 12 and 15 are located. They are polarized by the second dust cloud, that also belongs to the first sheet of absorption (Neckel & Klare 1980). Beyond that, the extinction keeps increasing to ∼1.2 kpc, where NGC 6250 is located. Behind the cluster, within 2 kpc, there is a region of transparency. Evidently, our polarimetric results are compatible with the work of Neckel and Klare.

Finally, not all of the observed stars could be plotted in this figure (e.g. 24 and 27) since their colour excesses are unknown. Therefore, we indicate their positions along the P_V axis to show that their polarization values are similar to those associated with the nearby star group.

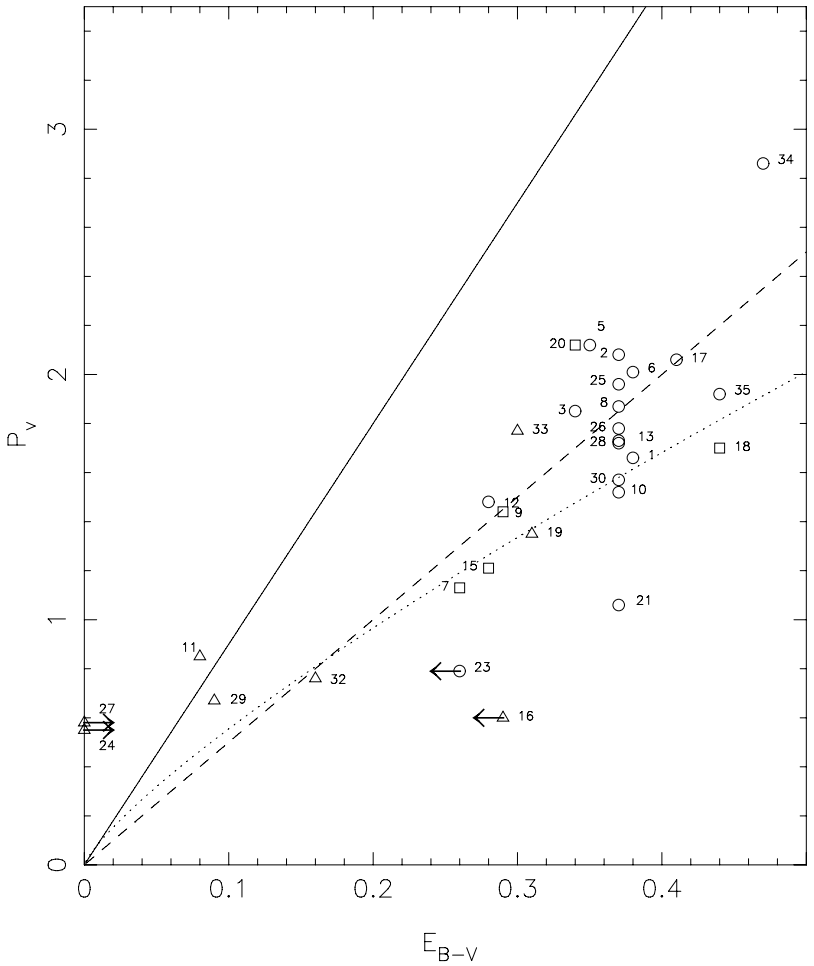

Figure 6. Plot P_V versus E_{B-V} for stars of NGC 6250. The solid line indicates $P_V = 9\ E_{B-V}$; the dashed line, $P_V = 5E_{B-V}$; and the dotted line, $P_V = 3.5E(B-V)^{0.8}$. Symbols are as indicated in Fig. 2.

5 SUMMARY

We have observed linear multicolour polarization for a sample of 32 stars in the region of the open cluster NGC 6250. The analysis of these data shows that the majority of the observed stars do not present indications of intrinsic polarization. The polarization efficiency, as indicated by the ratio $P_V/E_{B-V} = 4.95$, is normal when compared with the mean value of about 5 attributed to the ISM by Serkowski et al. (1975), but it is higher than the value predicted by Fosalba et al. (2002).

In the group of non-member stars, some of them are nearby stars (within 200 pc), but others are closer to the cluster (within 700 pc). In this region, we have been able to identify (polarimetrically) several dust components along the line of sight to the open cluster. The first component, located approximately within 300 pc of the Sun, polarizes the light from non-member stars and cluster members with an orientation dominated by the GP ($\sim 38^\circ$).

At least two more dust clouds are located between the nearby stellar group and the cluster, at distances between 300 and 700 pc for the first component and between 700 pc and 1 kpc for the second. Behind the cluster, there is a region of transparency, to $\sim$2 kpc and beyond that the extinction increases again as a consequence of the presence of another dust cloud. This last cloud is polarizing the light from star 34, located at a distance of greater than 2 kpc, according to photometric and polarimetric data. Our results are compatible with those of Neckel & Klare (1980). Finally, we have been able to identify an intracluster dust component, causing scattering in the measured polarization percentage and in the orientation of the vector $\boldsymbol{P}$ between the cluster members.

Once again, the polarization has proved to be a good criterion for determining and confirming star memberships of the stars in a cluster. In this study, we were able to confirm, clarify or adjust the membership status of several stars.

ACKNOWLEDGMENTS

We wish to acknowledge the technical support at CASLEO during the observing runs. We also acknowledge the use of the Torino Photopolarimeter built at Osservatorio Astronomico di Torino (Italy) and operated under agreement between CASLEO and Osservatorio Astronomico di Torino. We thank the referee Dr William Herbst for his thoughtful comments that helped to improve this manuscript.

REFERENCES

Axon D. J., Ellis R. S., 1976, MNRAS, 177, 499
Baumgardt H., Dettbam C., Wielen R., 2000, A&AS, 146, 251

Bayer C., Maitzen H. M., Paunzen E., Rode-Pauzen M., Sperl M., 2000, A&AS, 147, 99
Feinstein C., Baume G., Vergne M. M., Vázquez R., 2003a, A&A, 409, 933
Feinstein C., Martínez R., Vergne M. M., Baume G., Vázquez R., 2003b, ApJ, 598, 349
Fosalba P., Lazarian A., Prunet A., Tauber J., 2002, ApJ, 564, 762
Garrison R. F., Hiltner W. A., Schild R. E., 1977, ApJS, 35, 111
Goodman A. A., Bastien P., Myers P. C., Menard F., 1990, ApJ, 359, 363
Herbst W., 1977, AJ, 82, 902 (HW)
Houk N., Cowley A. P., Smith-Moore M., 1975, Catalogue of Two-Dimensional Spectral Types for the HD Stars, Vol. 1. Univ. of Michigan, Ann Arbor
Levenhagen R. S., Leister N. V., 2006, MNRAS, 371, 252
Maronna R., Feinstein C., Clocchiatti A., 1992, A&A, 260, 525
Martínez R., Vergne M., Feinstein C., 2004, A&A, 419, 965
Mathewson D. S., Ford V. L., 1970, Mem. R. Astron. Soc., 74, 139
McMillan R. S., 1978, ApJ, 225, 880
Moffat A. F. J., Vogt N., 1975, A&AS, 20, 155
Neckel Th., Klare G., 1980, A&A, 42, 251
Preston G. W., 1974, ARA&A, 12, 257
Scaltriti F., 1994, Technical Publication TP-001, Osservatorio Astronomica di Torino
Schmidt-Kaler Th., 1982, in Schaifers K., Voigt H. H., eds, Landolt-Borstein, Numerical Data and Functional Relationships in Science and Technology New Series, Group VI, Vol. 2. Springer-Verlag, Berlin, p. 1
Serkowski K., 1973, in Greenberg J. M., van de Hults H. C., eds, Proc. IAU Symp. 52, Interstellar Dust and Related Topics. Reidel, Dordrecht, p. 145
Serkowski K., Mathewson D. L., Ford V. L., 1975, ApJ, 196, 261
Van den Bergh S., Herbst W., 1975, AJ, 80, 208
Vergne M. M., Feinstein C., Martínez R., 2007, A&A, 462, 621
Whittet D. C. B., Martin P. G., Hough J. H., Rouse M. F., Nailey J. A., Axon D. J., 1992, ApJ, 386, 562
Wilking B. A., Lebofsky M. J., Martin P. G., Reike G. H., Kemp J. C., 1980, ApJ, 235, 905

This paper has been typeset from a TEX/LATEX file prepared by the author.